Water Research 245 (2023) 120672

Contents lists available at ScienceDirect

Water Research

journal homepage: www.elsevier.com/locate/watres

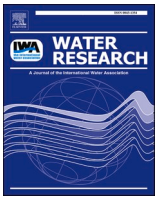

The role of ubiquitous metal ions in degradation of microplastics in hot-compressed water

Tan-Phat Vo [a], Jukka Rintala [a], Leilei Dai [b], Wen-Da Oh [c], Chao He [a,*]

[a] Materials Science and Environmental Engineering, Faculty of Engineering and Natural Sciences, Tampere University, Tampere, Finland
[b] Center for Biorefining and Department of Bioproducts and Biosystems Engineering, University of Minnesota, 1390 Eckles Ave., St. Paul, MN 55108, USA
[c] School of Chemical Sciences, Universiti Sains Malaysia, 11800 Penang, Malaysia

ARTICLE INFO

Keywords:
Hydrothermal processing
Microplastic degradation
Metallic catalyst
Free radicals
Resource recovery

ABSTRACT

Hydrothermal processing (HTP) is an efficient thermochemical technology to achieve sound treatment and resource recovery of sewage sludge (SS) in hot-compressed subcritical water. However, microplastics (MPs) and heavy metals can be problematic impurities for high-quality nutrients recovery from SS. This study initiated hydrothermal degradation of representative MPs (i.e., polyethylene (PE), polyamide (PA), polypropylene (PP)) under varied temperatures (180–300 °C) to understand the effect of four ubiquitous metal ions (i.e., Fe^{3+}, Al^{3+}, Cu^{2+}, Zn^{2+}) on MPs degradation. It was found that weight loss of all MPs in metallic reaction media was almost four times of that in water media, indicating the catalytic role of metal ions in HTP. Especially, PA degradation at 300 °C was promoted by Fe^{3+} and Al^{3+} with remarkable weight loss higher than 95% and 92%, respectively, which was ca. 160 °C lower than that in pyrolysis. Nevertheless, PE and PP were more recalcitrant polymers to be degraded under identical condition. Although higher temperature thermal hydrolysis reaction induced severe chain scission of polymers to reinforce degradation of MPs, Fe^{3+} and Al^{3+} ions demonstrated the most remarkable catalytic depolymerization of MPs via enhanced free radical dissociation rather than hydrolysis. Pyrolysis gas chromatography-mass spectrometry (Py GC–MS) was further complementarily applied with GC–MS to reveal HTP of MPs to secondary MPs and nanoplastics. This fundamental study highlights the crucial role of ubiquitous metal ions in MPs degradation in hot-compressed water. HTP could be an energy-efficient technology for effective treatment of MPs in SS with abundant Fe^{3+} and Al^{3+}, which will benefit sustainable recovery of cleaner nutrients in hydrochar and value-added chemicals or monomers from MPs.

1. Introduction

Plastic products have become indispensable in our daily life due to their excellent durability, anti-degradation, and low manufacturing cost. However, plastics are one of the most severe environmental pollutants in the world (Wang et al., 2022a). Especially, microplastics (MPs) (plastic particles smaller than 5 mm in size) could pose threat to the environment (Torres et al., 2021). MPs can enter human body by inhaling polluted air and ingesting contaminated food and water (Collivignarelli et al., 2021). MPs are ubiquitous in the environment and can be found in marine and continental waters (Mao et al., 2020), marine sediments (De-la-Torre et al., 2020), terrestrial and agricultural environments (Dioses-Salinas et al., 2020), even in polar regions (Lusher et al., 2014). Recent studies have indicated that sewage sludge (SS) from wastewater treatment plants (WWTP) contains a large amount of MPs (Li et al., 2018). The concentration of MPs in SS ranges from 1.60×10^3 to 56.4×10^3 particles per kg dry sludge (Li et al., 2018). In general, MPs found in SS include polyethylene (PE), polyamide (PA), polypropylene (PP), polyvinyl chloride (PVC) and polystyrene (PS) (Collivignarelli et al., 2021). More specifically, the MPs are mainly composed of fibers (75.8%), fragments (18.5%), films (1.9%), other unidentified particles (~1.2%) (Mahon et al., 2017).

In addition to MPs, inorganic metallic impurities are widely found in SS, such as heavy metals (e.g., Cu, Ni, Cr and Pb) originating from wastewater and metallic salts (e.g., polyaluminum chloride, ferric chloride) from added chemicals during wastewater treatment (Chanaka Udayanga et al., 2018; Wang et al., 2022b). For instance, in Finland, the application of Al and Fe coagulants in WWTP increases the metal ion concentration, leading to a high concentration of Fe (17,200 mg/kg dry matter (d.m.)) and Al (629 mg/kg d.m.) followed by Cu (138 mg/kg d.

* Corresponding author.
E-mail address: chao.he@tuni.fi (C. He).

https://doi.org/10.1016/j.watres.2023.120672
Received 1 May 2023; Received in revised form 2 August 2023; Accepted 25 September 2023
Available online 26 September 2023

m.), Zn (30 mg/kg d.m.), Mn (28 mg/kg d.m.) and Ti (19.0 mg/kg d.m.) (Pöykiö et al., 2019). The presence of metals in the form of ions is often observed in association with organic matter. However, certain metals and inorganic salts in SS can lead to precipitates, such as sulfides, oxides, and phosphonates (Geng et al., 2020). Release of metal ions from SS into the environment via SS disposal, such as land application, building materials and sanitary landfill, has the potential to impact the food chain at all levels, from microorganisms, to plants, animals, and ultimately human beings (Alengebawy et al., 2021; Geng et al., 2020).

The investigation of mixed MPs in SS has revealed their interactions with organic pollutants, antibiotics, and microorganisms (Mahon et al., 2017; Torres et al., 2021). Specifically, metal ions are absorbed onto the MPs due to their porous surfaces and negative charges (Gao et al., 2019; Torres et al., 2021), leading to persistent presence of MPs and metal ions in the environment over an extended period of time (Brennecke et al., 2016). This coexistence has been reported in biofuels from thermochemical conversion, including hydrochar (Han et al., 2022) and biochar (Li et al., 2022a). Particularly, MPs may be still present in biochar from pyrolysis below 500 °C. Both metal elements and secondary MPs were observed in biochar after pyrolysis at 500 °C (Ni et al., 2020). Hydrothermal processing (HTP) achieved about 50% and 87% removal rate of tiny MPs in SS within 30 min at 170 °C and 220 °C, respectively (Jiang et al., 2022).

HTP has been widely applied as a promising solution to the disposal of SS for resource and energy recovery with minimized environmental risks (Li et al., 2022b). HTP has also been attempted to degrade MPs in SS owing to its avoidance of pre-drying and lower energy consumption as compared to conventional pyrolysis and gasification techniques (Jin et al., 2021). Previous studies have demonstrated that HTP can effectively degrade MPs in SS, with 79% destructed after treatment at 260 °C (Xu and Bai, 2022), whereas 99% degradation was achieved using pyrolysis at 450 °C (Ni et al., 2020). Moreover, HTP emitted less exhaust gases than pyrolysis during MP degradation (Ni et al., 2020). Although there are some recent studies on HTP of MPs in SS (Jiang et al., 2022; Li et al., 2022b; Xu and Bai, 2022), the degradation or destruction of MPs was not obvious. Moreover, those earlier hydrothermal studies were generally conducted under temperature lower than 260 °C. This HTP temperature may be too low for MPs degradation because significant destruction of MPs was only observed at higher temperature of 450 °C in conventional pyrolysis of SS (Ni et al., 2020). More importantly, the high heterogeneity and complexity of chemical composition in SS make it extremely difficult to differentiate the effect of hydrothermal treatment on the transformation of MPs from that of other organic substances (e.g., carbohydrates, lipids and proteins) (Li et al., 2022b). In addition, the coexistence of organic matter could also interfere the analysis of MPs in SS, causing potential bias on the determination of MPs therein. Although metal ions may play a critical role in degradation of MPs in SS, this effect has not been systematically explored. After hydrothermal carbonization of plastics in seawater from 220 to 300 °C, effective decomposition of plastics commenced at 250 °C with hydrochar from 300 °C exhibiting the most significant degradation of plastics (Iñiguez et al., 2019). This may imply that metal ions in seawater may affect the degradation of plastics. Under the global context of ever-increasing MPs pollution in water environment and SS, it is imperative to implement fundamental study to acquire in-depth and holistic knowledge on the hydrothermal degradation behavior of MPs in hot-compressed water, especially in the presence of ubiquitous metal ions emerging in SS.

Therefore, this study aims to unravel the interaction of ubiquitous metal ions and MPs in hot-compressed water on the degradation of MPs in terms of hydrothermal temperature, chemical composition and physical properties of MPs, and reaction media. Ultimately, the study will provide insights into the role of metal ions in the degradation of MPs and elucidate the hydrothermal degradation pathways of MPs in the presence of these metal ions.

2. Materials and methods

2.1. Materials

Three typical MPs in SS, including PE, PP, PA, were selected for HTP. High-density PE, PP microspheres, and PA 6 fiber were purchased from Cospheric LLC and Flocking Company (U.K.). To investigate HTP of various MPs with different sizes and shapes, PE and PP fragments were further prepared by manual grinding and crumbling (Fig. S1). According to the average diameter of MPs detected in SS (Raju et al., 2020), MPs with sizes ranging from 100 to 500 μm were screened for experiments. Table 1 summarizes the elemental composition and dimensions of all five MP samples. Copper (II) nitrate ($Cu(NO_3)_2$), iron (III) nitrate ($Fe(NO_3)_3$), aluminum nitrate ($Al(NO_3)_3$), and zinc nitrate ($Zn(NO_3)_2$) were used to prepare four metallic solutions using Milli-Q water with a metal ion concentration of 2.37 g/L, 2.17 g/L, 0.88 g/L and 2.41 g/L, respectively.

2.2. Experimental

HTP of different MP samples was performed in a 125 mL hydrothermal autoclave with a modified stainless-steel liner (Series 4748, Parr Instrument, USA) (Fig. S2). Approximately 30–40 mg of individual MP was mixed with 25 mL of water or metallic solution separately, which was fed into the reactor vessel and sealed tightly for hydrothermal reactions. The reactor was then placed in an oven to heat up to pre-set temperature at 10 °C/min and maintained for a residence time of 30 min. Different applied temperatures were 180, 210, 240, 270 and 300 °C with autogenous pressure of 10.0, 19.0, 33.5, 55.0 and 85.9 bar, respectively. The liquid and working volume ratio was calculated to ensure desired autogenous pressure with sufficient safety (Ro et al., 2020). After reaction, the reactor was cooled to room temperature. The collected mixture was separated into solid and aqueous phases by filtration through a 26 μm stainless steel mesh. The solid phase was washed with 50 mL Milli-Q water and oven-dried at 60 °C for 2 h to collect MP residues. Afterwards, the MP residues were weighted and used for elemental analysis (Fig. S3). The aqueous phase was partly evaporated overnight at 60 °C to collect the solute for further analysis and characterization. Weight loss of MPs was determined by the weight before and after HTP using the equation below. The MP residue was denoted as M-X, where M represents the type of MP and X indicates the hydrothermal temperature. For example, PEs-180 and PP-300 stand for the MP residues from HTP of PEs under 180 °C, and PP under 300 °C, respectively. The schematic diagram of HTP procedure is described in Fig. 1.

$$\text{Weight loss} = \frac{W_0 - W_t}{W_0} \times 100\ \%$$

Where W_0 and W_t is the weight of MPs before and after the HTP, respectively.

Table 1
Physicochemical properties of different microplastic samples.

Microplastic samples	Dimension	Elemental composition (wt%)			
		C	H	N	O
PE sphere (PEs)	Diameter: 150–180 μm	83.16	14.20	0.03	1.84
PE fragment (PEf)	Diameter: 425–500 μm	84.14	13.30	0.07	1.74
PA fiber (PA3)	Length: 3.0 mm, Diameter: 70 μm	62.37	9.38	10.67	16.85
PA fiber (PA5)	Length: 5.0 mm, Diameter: 110 μm	62.96	9.92	11.55	14.88
PP fragments	Diameter: 100–500 μm	85.14	14.11	0.04	0.04

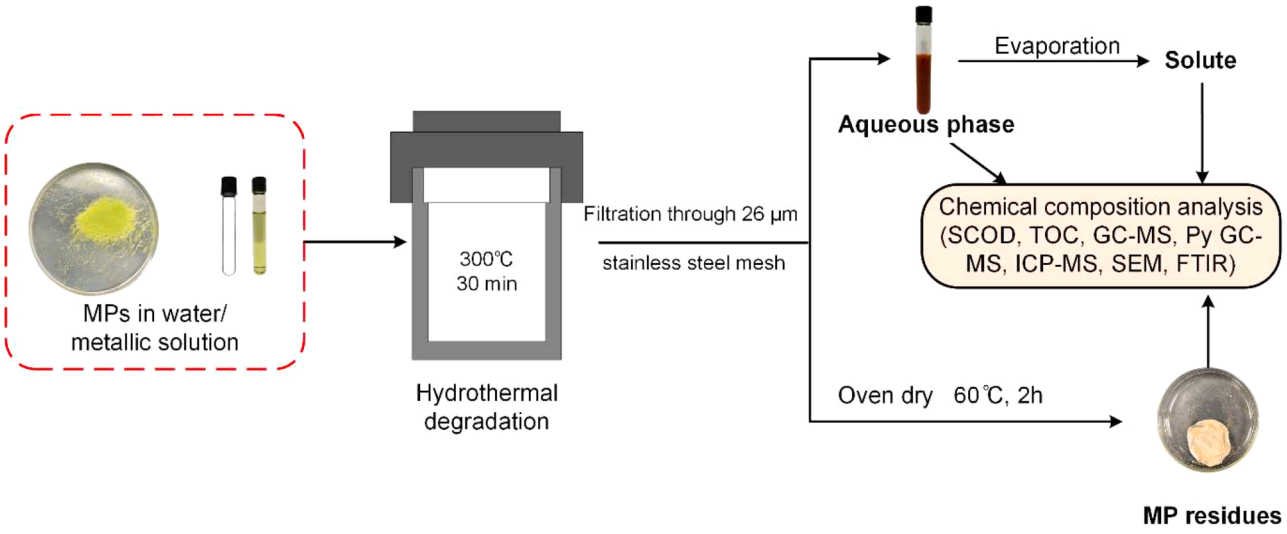

Fig. 1. The schematic diagram of HTP of MPs in water and metallic solution and analytical techniques for various products.

2.3. Analytical methodologies

2.3.1. Characterization of MPs and residues

Thermogravimetric analysis (TGA) was used to study the thermal stability of pristine MPs using Shimadzu TGA 50 equipped with a TA 50WSI thermal analyzer. Briefly, pyrolytic degradation of MPs was conducted within 100–900 °C at 5 °C/min with a flow of 20 mL/min high-purity nitrogen gas. The pyrolytic degradation of MPs was characterized by three representative temperatures, including starting (T_s), maximum (T_m) and ending (T_e) temperature. C, H, N and O contents in MP residues were determined using elemental analyzer (OEA, Thermo Scientific FlashSmart Elemental Analyser). The surface morphology of MP residues after HTP in metallic media was examined using JEOL IT-500 scanning electron microscopy (SEM) operating at 5 kV under a low vacuum mode (10–20 Pa). Metal ions adsorbed on the surface of MP residues were determined using inductively coupled plasma mass spectrometry (ICP-MS) (Thermo Scientific iCAP™ RQ) equipped with a concentric Nebulizer after microwave digestion in nitric acid.

2.3.2. Physicochemical analysis of aqueous phase

Soluble chemical oxygen demand (SCOD) of aqueous phase was determined following standard methods (Apha, 2007). Total organic carbon (TOC) of aqueous phase was measured using Shimadzu TOC-VCPH. Chemical composition of aqueous phase was determined using a Shimadzu Nexis GC-2030 gas chromatography-mass spectrometry (GC–MS) equipped with a ZB-WAXplus™ column (30 m × 0.25 mm × 0.25 μm) at 250 °C. Furthermore, a single shot pyrolysis GC–MS (Py GC–MS) (EGA/PY-3030 D) was used to obtain more accurate chemical composition information of the solute from aqueous phase after HTP. After pyrolysis at 600 °C, the evolved volatiles could be analyzed by a coupled GC–MS equipped with an Ultra ALLOY column. The analysis was performed at injection temperature of 360 °C with high-purity helium as carrier gas. NIST (National Institute of Standards and Technology, Gaithersburg, MD, USA) mass spectral database was used for chemical identification. Polymers in the solute was detected by using a Fourier-transform infrared spectroscopy (FTIR) (Spectrum Two FTIR Spectrometer L1600300). The instrument was operated in single reflection mode with a speed of 5 kHz, a resolution 4 cm and a mid-IR range of 600 and 4000 cm^{-1}.

3. Results and discussion

3.1. Comparative degradation of different MPs

3.1.1. Pyrolytic degradation of MPs

Thermal stability of all pristine MPs (i.e., PEs, PEf, PA3, PA5 and PP) was studied using TGA to determine their pyrolytic profiles (Fig. 2) and corresponding characteristic temperatures. Fig. 2 depicts the weight loss (TG) and weight loss rate (DTG) curves for pyrolysis of MPs. All MPs showed a single-stage degradation profile, despite varying temperature ranges. The type of MPs distinctly affected their pyrolytic profile. PA, including PA3 and PA5, exhibited a wide degradation range of 330–500 °C with T_m around 460 °C, while PE (i.e., PEs and PEf) and PP showed a narrower degradation range of 360–508 °C and 420–490 °C with T_m of ca. 485 °C and 474 °C, respectively (Fig. 2 and Table S1). This finding confirms that conventional pyrolysis could only destruct more than 95% of MPs (e.g., PA, PE, PP) in SS when the temperature was above 450 °C (Ni et al., 2020). The different thermal degradation profiles of MPs were associated with intrinsic chemical compositions and structures. PA degradation was induced by random or nearly random chain scission and β-C–H hydrogen-transfer reaction (Pannase et al., 2020), while PE and PP were decomposed by random scission of the durable main chain (Ellis et al., 2021). Furthermore, this study suggests that the size of MPs had slight effect on the characteristic temperatures with difference of less than 10 °C in pyrolytic degradation, especially T_s of 330 °C and 335 °C for PA3 and PA5, T_s of 360 °C and 368 °C for PEs and PEf, respectively (Fig. 2 and Table S1). Thus, easier degradation can be expected for the same type of MPs with smaller size.

3.1.2. Hydrothermal degradation of MPs

Hydrothermal degradation efficiency of MPs was quantified in terms of weight loss, SCOD and TOC in Fig. 3. On the whole, PA was prone to be degraded with the highest degradation efficiency followed by PE and PP. Regardless of the reaction media, higher temperature generally facilitated the degradation of all five MPs. Besides, degradation of MPs in metallic media was more favorable than that in water media, while improved degradation was found for MPs (e.g., PE and PA) with smaller particle size.

3.1.2.1. Effect of temperature. Higher temperatures could induce severe depolymerization and lead to enhanced hydrolysis and degradation of MPs in both metallic and water media, which was indicated by increasing SCOD and TOC concentrations of aqueous phase. When the temperature was lower than 240 °C, weight loss of all MPs was less than

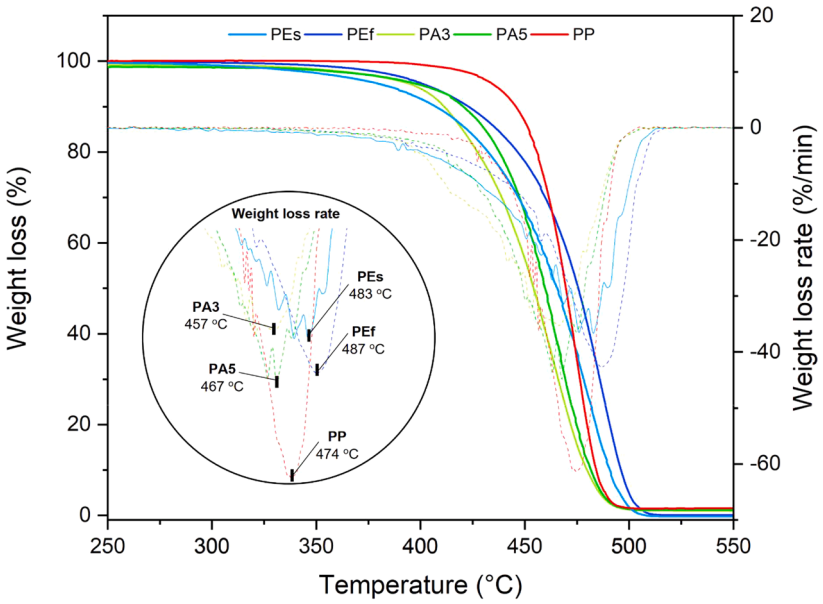

Fig. 2. TG and DTG curves for pyrolytic degradation of different MPs.

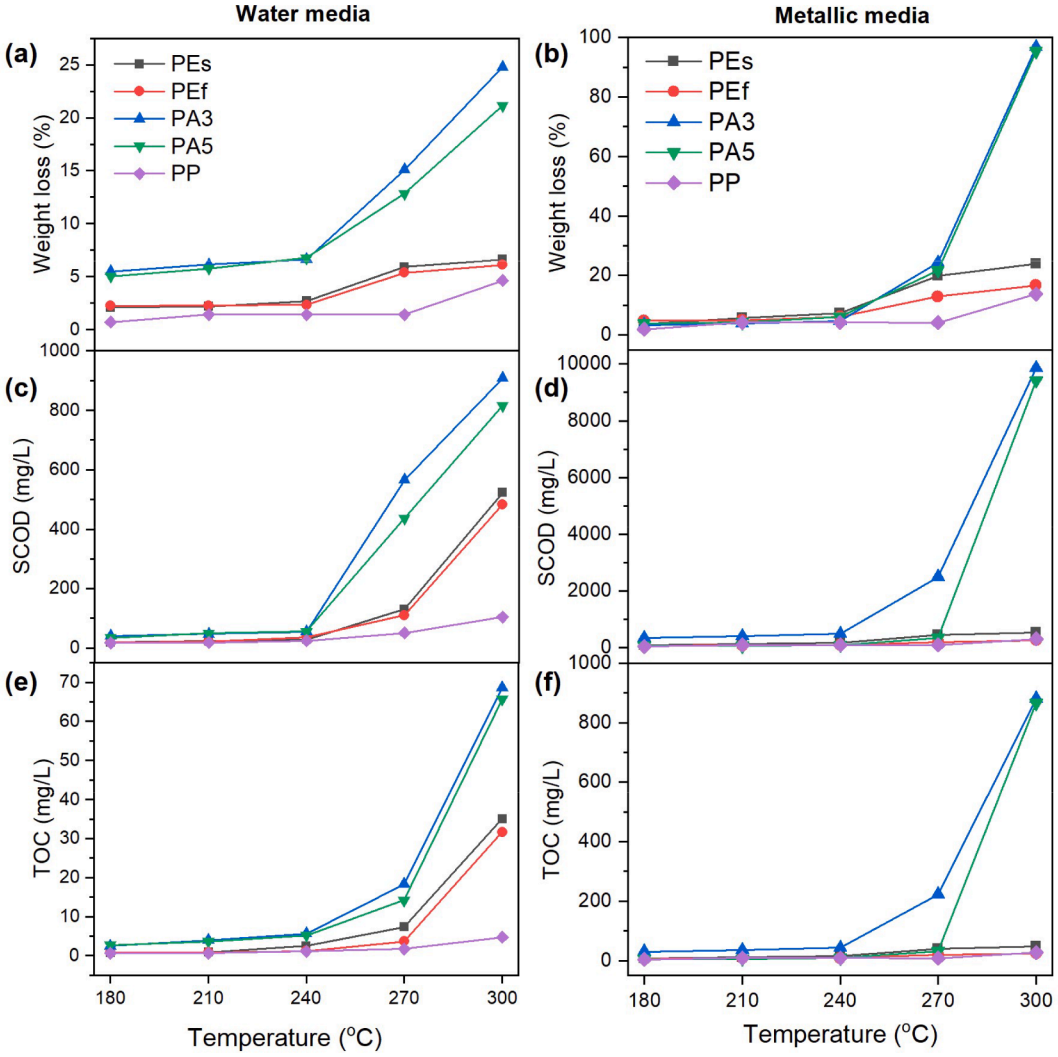

Fig. 3. Comparative weight loss of different MPs, SCOD and TOC of aqueous phase after hydrothermal degradation in water media (a, c, e) and metallic media (b, d, f) under various temperatures.

5% in water media but achieved 10% in metallic media. After HTP at 300 °C, the highest weight loss was found for all MPs, which was increased by nearly four-fold. Specifically, after HTP of PA3 in metallic media, a weight loss of 7% at 180 °C was dramatically increased to more than 95% at 300 °C which was about 160 °C lower than T_m for PA3 in pyrolytic degradation. Meanwhile, the concentrations of SCOD and TOC in the aqueous phase were increased from 337.2 mg/L and 30.2 mg/L at 180 °C to 9854.6 mg/L and 880.5 mg/L at 300 °C, respectively.

However, the effect of temperature on MP degradation was less notable for PE and PP. After HTP in water media, the weight loss, concentration of SCOD and TOC of aqueous phase for PEs and PEf were ca. 2.5%, 18.8 mg/L and 0.8 mg/L at 180 °C, which were increased to 6.1% and 6.9%, 523.5 and 483.3 mg/L, 35.4 and 31.6 mg/L at 300 °C, respectively. PP had the lowest weight loss (0.7%), SCOD concentration (16.9 mg/L), and TOC (0.6 mg/L) at 180 °C, which were increased to 4.6%, 103.5 mg/L and 4.6 mg/L, respectively, at 300 °C (Fig. 3). Under HTP, temperature increases the self-diffusion coefficient of water to improve its molecular mobility and thus enhance its penetration into plastic polymers (Xu and Bai, 2022). At higher temperature, hydrogen atoms are detached from polymer chain to induce unstable MPs (Hu et al., 2021; Xue et al., 2017) which can be hydrolyzed by subcritical water in HTP. Subcritical water attacks the unstable bonds of MPs, leading to degradation (Zhao et al., 2018). A recent study also validated that higher temperature notably facilitated hydrothermal degradation of MPs (e.g., PE, PA, PP) in SS under 180 to 260 °C with a maximum degradation of 79% at 260 °C (Xu and Bai, 2022).

3.1.2.2. Effect of different MP properties. The hydrothermal degradation of MPs was not only affected by the temperature, but also the chemical composition as well as the sizes and shapes of MPs. Among all MPs, PA exhibited the highest weight loss corresponding to the highest concentrations of SCOD and TOC as compared to those of PE and PP under identical temperature and media (Fig. 3).

The chemical composition of MPs reflects its inherent chemical properties, especially their resistance and durability under various environmental conditions, including temperature and chemical exposure. In this study, PA displayed a higher severity of hydrothermal degradation, while PE and PP exhibited greater resistance at equivalent temperature and media conditions. PA3 and PA5 indicated the highest weight loss, SCOD and TOC as compared with PEs, PEf and PP under the same temperature and media. After HTP at 270 °C in water media, the weight loss of PEs and PP was around 5.9% and 2.4%, respectively, while that of PA5 was 13.8%. The difference was the most remarkable at 300 °C in metallic media, where the weight loss of PA5 (95.3%) was remarkably higher than that of PEs (23.8%) and PP (13.6%), resulting in distinctly different concentrations of SCOD and TOC for PA5 (9418.9 and 565.3 mg/L), PEs (527.5 and 47.1 mg/L) and PP (303.2 and 27.9 mg/L) (Fig. 3). It can be deduced that PA is relatively sensitive to temperature due to its intrinsic chemical structure (Ellis et al., 2021). On the other hand, PE and PP belong to the polyolefin family, which are considered refractory to degradation due to their intrinsic stable hydrocarbon skeletons (Ellis et al., 2021). Our present study showed that PA, PE and PP remained after HTP at 270 °C in both media, whereas only PE and PP were determined in hydrochar from HTP of SS at 260 °C (Xu and Bai, 2022). This difference may be explained by the evolution of chemical properties for pristine and aged MPs in SS. MPs undergo multiple processes in WWTPs, ending up with increased carbonyl index and surface area, and changed color. These aged MPs exhibited lower temperature resistance than that of pristine MPs (Luo et al., 2020). Furthermore, size and shape of MPs also affected the hydrothermal degradation and depolymerization through interaction of subcritical water and MPs in thermal hydrolysis. It is supposed that HTP substantially reduced MPs size at higher temperature (Jiang et al., 2022). MPs with smaller dimensions were prone to degradation. For example, PEs and PA3 showed higher weight loss, SCOD and TOC than PEf and PA5 at all temperatures (Fig. 3).

3.1.2.3. Effect of reaction media. As shown in Fig. 3, all five MPs only exhibited slight degradation with a weight loss of less than 20% at lower temperatures (180–270 °C) in both water and metallic media. More specifically, at 270 °C, the weight loss of PEs, PEf and PP was around 5.9%, 5.3% and 2.0% in water media and exceeded 19.8%, 12.8% and 4.0% in metallic media with SCOD of 129.8, 110.4 and 50.1 mg/L in water media, and that of 439.9, 204.7 and 91.8 mg/L in metallic media, respectively.

On the other hand, when the temperature increased to above 270 °C, metal ions started to facilitate a distinct weight loss for all MPs. Especially the weight loss was even higher than 95% for PA3 and PA5 at 300 °C, followed by ca. 17% for PEs and PEf, and 13% for PP. However, this was about 24% for PA3, less than 5% for PEs, PEf and PP in water media. This reveals that metallic media could enhance the hydrothermal degradation of MPs by more than three times that in water media. Consequently, a remarkable increase in SCOD and TOC was determined in the aqueous phase.

In general, the degradation of MPs under HTP occurred mainly via thermal hydrolysis by free radicals (•H and •OH) (Jiang et al., 2022). Particularly, high concentration of generated •H partially broke down polymer structures of MPs, while •OH primarily destructed chemical bonds in MPs during hydrothermal Fenton process (Hu et al., 2021). Since metal ions (Fe^{3+}, Al^{3+}, Zn^{2+} and Cu^{2+}) enhanced MP degradation, it is postulated that these metal ions could increase free radicals in the hydrolysis process that contributed to MP degradation. With the increment of HTP temperature, more free radicals can be generated to intensify the depolymerization, which might further explain the increased weight loss of all MPs in two reaction media when the temperature reached 300 °C. In addition, the adsorbed metal ions on MPs and the morphology of MPs after the HTP were examined in Figs. S4 and S5, revealing that metal ions not only facilitated hydrothermal degradation of MP but also were adsorbed on MPs with a low concentration (<10% of total metal ion concentration). Thus, this promoting effect of metal ions on the degradation of MPs led to the hypothesis that metal ions could function as catalysts in hydrothermal process.

3.1.2.4. Evolution of chemical composition of MP residues from HTP. Van Krevelen diagram in Fig. 4 is applied to visualize the evolution of hydrogen/carbon (H/C) and oxygen/carbon (O/C) atomic ratios of MP residues from HTP under various conditions (i.e., reaction media, reaction temperature and different types of MPs). This could indicate different reaction pathways (Fig. 4a) during HTP, including dehydration, decarboxylation and demethanation.

Based on their inherent chemical composition of all MPs, pristine PE and PP exhibited similar H/C and O/C atomic ratios, but pristine PA showed a high O/C atomic ratio. With the increase of reaction temperature during HTP in water media, a dramatic decrease of H/C and O/C atomic ratios was found in residues of PE and PP. In contrast, PA residue presented only a negligible decrease in H/C atomic ratio but a noticeable decrease in O/C atomic ratio.

As indicated in Fig. 4b, PA experienced decarboxylation and dehydration reactions with the increased temperature under both media, decreasing O/C and H/C atomic ratios. More specifically, O/C ratio of PA residue decreased from 0.2878 at 180 °C to 0.2716 at 300 °C in water media, and from 0.2882 at 180 °C to 0.2846 at 270 °C in metallic media, while there was an insignificant reduction of H/C ratio after HTP at 180–300 °C in both media. Notably, the disappearance of PA-300 in metallic media (Fig. 4b) was attributed to 95% of weight loss. The decrement in atomic contents could mainly result from MPs depolymerization into monomers via hydrothermally reinforced hydrolysis (Wang et al., 2015). The major reduction O/C in comparison with H/C in PA residue may be due to the cleavage of peptide bond and N-alkyl amide that can be easily scissored under thermal hydrolysis (Dümichen

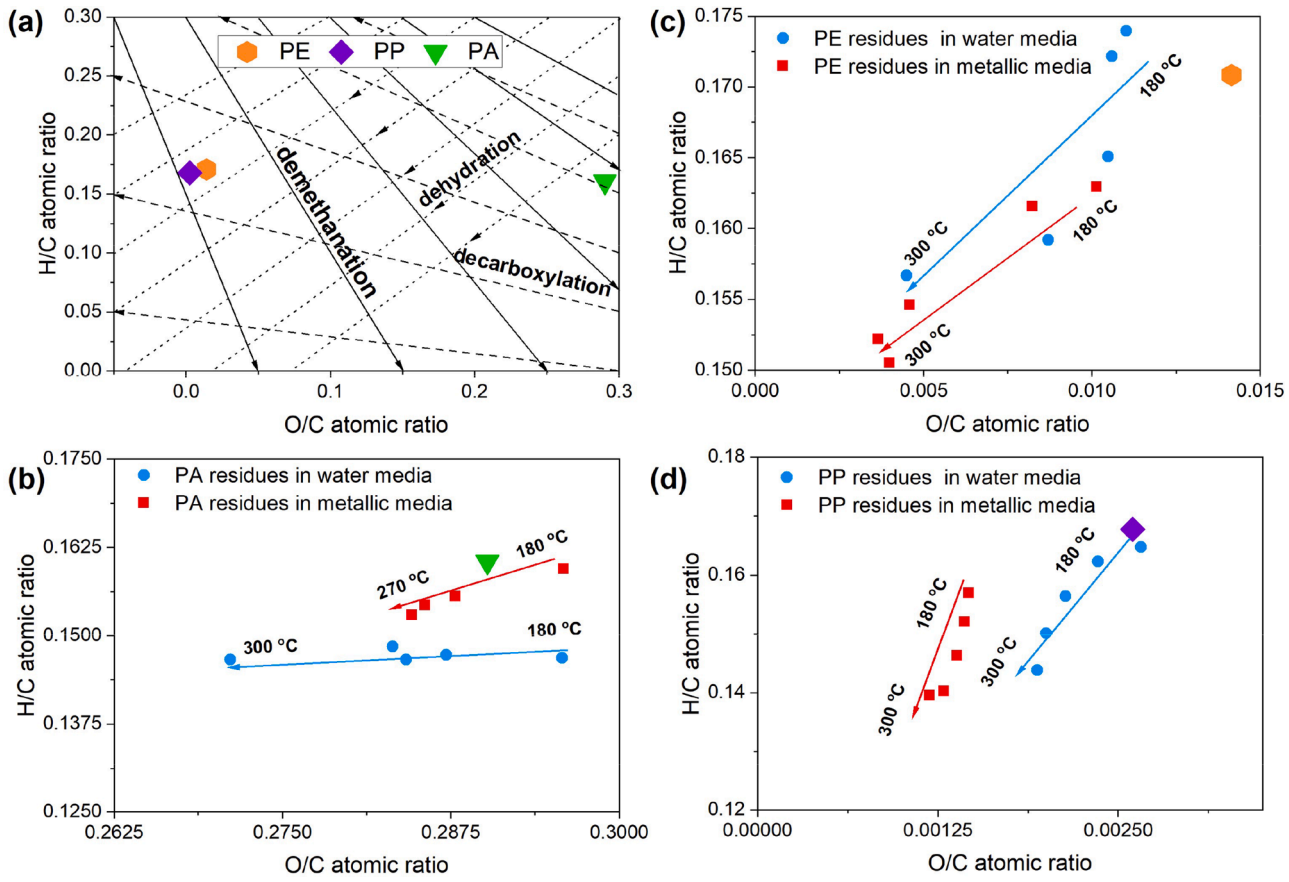

Fig. 4. Van Krevelen diagram of (a) pristine MPs, (b) PE, (c) PA, and (d) PP after HTP at different media and temperatures.

et al., 2017). On the contrary, dehydration was predominant in HTP of PE and PP with elevated temperature, exhibiting a remarkable reduction of H/C but limited decrement of O/C originating from the absence of O in their chemical composition. When HTP temperature was elevated from 180 to 300 °C, H/C atomic ratio in PE residue decreased from 0.175 to 0.155 in water media, and from 0.165 to 0.150 in metallic media. When the temperature was increased from 180 to 300 °C, despite a similar decreasing trend with that for PE residue in both media (Fig. 4c and d), H/C ratio in PP residue demonstrated a sharp reduction, especially in metallic media, implying a higher temperature sensitivity of PP in HTP. This reduction of H/C in PE and PP residues could be related to their inherent chemical structure where hydrogen atom therein is directly linked to a carbon backbone instead of other functional groups (Dümichen et al., 2017; Li et al., 2022b). Moreover, C—H bond in PE and PP is more durable than C—N and C—O bonds under identical condition (Ellis et al., 2021), coinciding with a higher degradation efficiency of PA than that of PE and PP during HTP in both media. Hence, it is concluded that decarboxylation and dehydration dominated the HTP of PA, whereas dehydration was a more favorable reaction for PE and PP. Notably, metallic media could distinctly improve their depolymerization and PP was more readily decomposed than PE under higher HTP temperature.

3.2. Catalytic role of metal ions in HTP of MPs

To investigate the effect of different metal ions on the degradation of MPs, 1 g/L of four metallic solutions (i.e., $Fe(NO_3)_3$, $Cu(NO_3)_2$, $Zn(NO_3)_2$ and $Al(NO_3)_3$) were individually employed in HTP at 300 °C for 30 min. Overall, Fe^{3+} was the most advantageous in degradation of three MPs over Cu^{2+}, Zn^{2+} and Al^{3+}. Regardless of the different metal ions, PA showed a remarkable weight loss with the highest SCOD and TOC compared to PE and PP under identical conditions (Fig. 5), which could be associated with the inherent structural stability of MPs. Generally, hydrothermal degradation of MPs could be affected by free radical reaction (Yin et al., 2011), chemical structures of MPs (Ellis et al., 2021) and hydrothermal conditions (e.g., temperature, pressure) (Xu and Bai, 2022). Besides, metal ion was another factor to promote or inhibit HTP. The degradation severity for HTP of MPs was previously found to be closely related with the chemical composition of MPs, hydrothermal temperature, and free radical reaction. Nonetheless, the present study confirmed the crucial role of metal ions in HTP of MPs.

3.2.1. Effect of individual metal ion on degradation of MPs

As depicted in Fig. 5, Fe^{3+} and Al^{3+} media distinctly facilitated hydrothermal degradation of PA with more than 95% and 92% of weight loss, respectively, resulting in corresponding SCOD of 9537 mg/L and 9463 mg/L, TOC of 876 mg/L and 845 mg/L, respectively. However, the weight loss of PA was less than 20% in Cu^{2+} and Zn^{2+} media, leading to reasonably lower concentrations of SCOD and TOC. PA is a condensation polymer, so hydrolysis is the primary route for depolymerizing condensation polymers (Xu and Bai, 2022). In particular, the peptide bond and N-alkyl amide of PA can be easily scissored by free radicals generated from hydrothermal hydrolysis (Jiang et al., 2022). Meanwhile, due to strong ion exchange capacity, Fe^{3+} and Al^{3+} may get involved in the redox reaction with water to generate more hydroxyl radicals, thereby promoting hydrothermal degradation of PA. In contrast, the degradation of PA was insignificant in Cu^{2+} and Zn^{2+} media with markedly lower weight loss of 15.2% and 19.5%, respectively (Fig. 5). Actually, Cu^{2+} and Zn^{2+} have been reported to increase PA stabilization in homogeneous catalytic thermal degradation (Cerruti and Carfagna, 2010). The discrepancy between $Fe^{3+}/Al^{3+}$and Cu^{2+}/Zn^{2+} in PA degradation could be attributed to the affiliation of

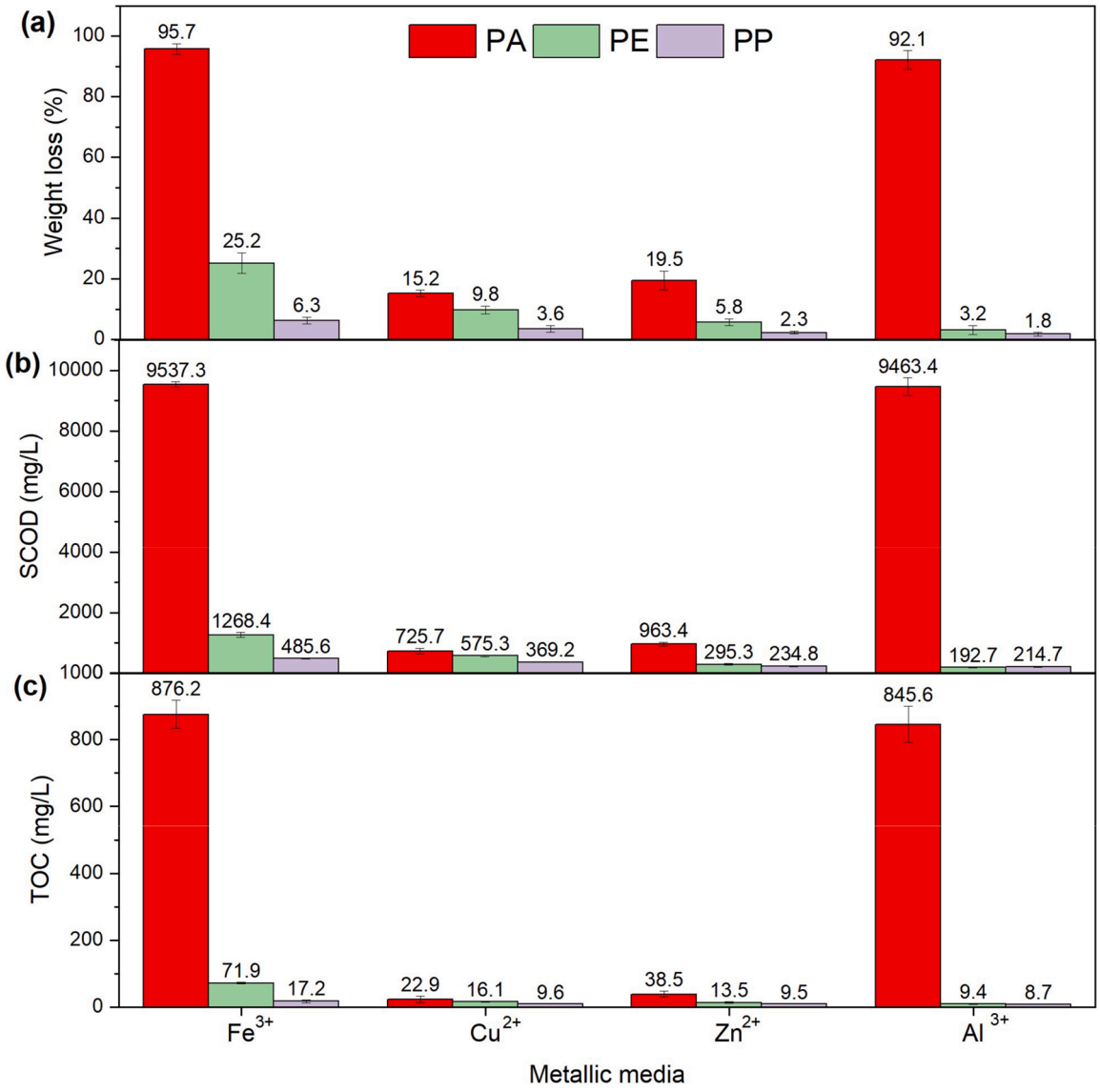

Fig. 5. Evolution of (a) mass loss, (b) TOC and (c) SCOD of PA, PE and PP after HTP at 300 °C in different individual metallic media (i.e., Fe^{3+}, Cu^{2+}, Zn^{2+} and Al^{3+}).

metal ions with chemical composition of PA and the redox capability to enhance free radical generation. It can therefore be assumed that Fe^{3+} and Al^{3+} acted as favorable catalysts in PA degradation.

Nevertheless, the degradation of PE and PP was relatively insignificant in all metallic solutions. Even in the presence of Fe^{3+}, the weight loss of PE and PP was only ca. 25% and 6%, respectively, while higher resistance to degradation was observed for other metallic media (Fig. 5). In fact, degradation of PE and PP is challenging due to the lack of functional groups in their hydrocarbon skeletons and high C—H bond energy (414 kJ/mol) (Zhao et al., 2018). It seems that hydrolysis has less effect on PE and PP degradation. To facilitate degradation, higher reaction temperature or additional catalysts are required (Ellis et al., 2021). Thus, in this study, metal ions, such as Fe^{3+}, Cu^{2+}, Zn^{2+}, and Al^{3+}, can be introduced as catalysts to improve the degradation. The weight loss of PE and PP in the presence of these metal ions was higher than that in water media. This phenomenon can be attributed to the strong hydration effect of metal ions that leads to hydroxyl substitution in the polymer chain. This substitution then caused the affiliation of hydroxyl groups with water molecules, resulting in the scission of plastic polymers into smaller units or monomers (Ma et al., 2021). Although there is still a lack of conclusive evidence on effective catalysts for PE and PP degradation, Fe^{3+} was more advantageous than other three metal ions in this study.

3.2.2. *Degradation products in aqueous phase*

FTIR spectra in Fig. 6 were used to analyze the functional groups of degradation compounds in different solutes of aqueous phase from HTP of MPs. Generally, MP solutes from Fe and Al media (type I) demonstrated similar FTIR spectra patterns, and those from Cu and Zn media (type II) were comparable. For instance, peaks at 1450–1440 cm^{-1} (C—H bending) and 1290 – 1270 cm^{-1} (C—O bending) showed comparable intensities for PA solutes from type I, while those from type II exhibited similar peak intensities. This implies similar degradation products in these two types of media, which was also evidenced by Py GC–MS data summarized in Table S3. Based on the spectra comparison between pristine MPs and MP solutes, peaks at 2950 – 2840 cm^{-1} (CH_2 stretching) for pristine MPs were altered to a board peak at 3395 cm^{-1} which was ascribed to O—H stretching of hydroperoxide resulting from the association of H_2O molecules with polymers during HTP (Jiang et al., 2022). Besides, different peaks at 1650 – 600 cm^{-1} corresponding to various functional groups (e.g., C—H, C—O, C—O—C) were attributed to degradation products of MPs. Nevertheless, FTIR spectra did not reflect the existence of remaining smaller MPs in the solutes. Additional comprehensive techniques, including GC–MS and Py GC–MS, are

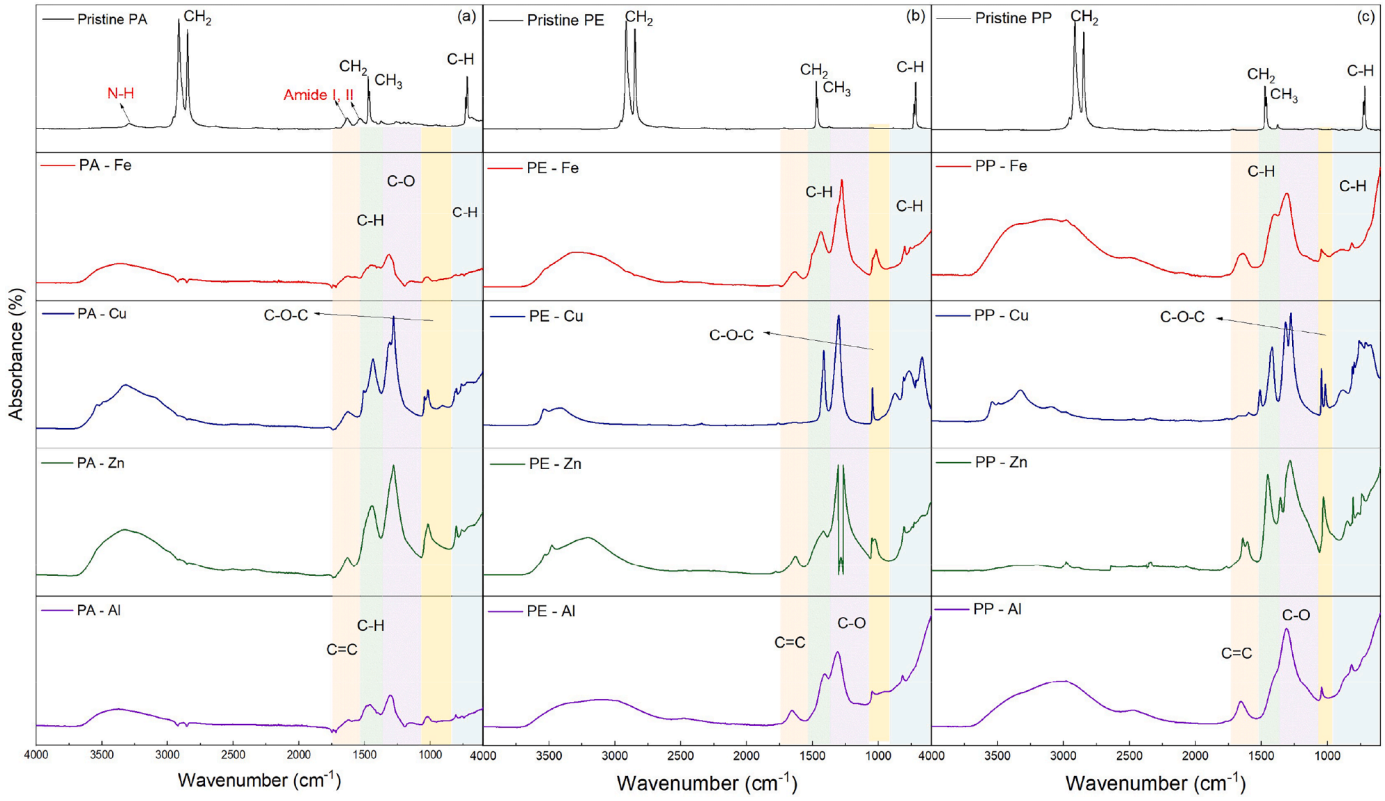

Fig. 6. FTIR spectra of pristine MPs and their different solutes from HTP.

essential to ensure accurate and complete characterization of MPs degradation products from HTP.

Subsequently, GC–MS and Py GC–MS were further applied to comprehensively analyze derived organic components in aqueous phase and corresponding solute, respectively. Fig. 7 depicts the relative abundance of organics in aqueous phase using GC–MS. The degradation products of PA implied the degradation routes using different metal ions. 5-hexenoic acid was found to be the most abundant, followed by caprolactam (CPL), ammonium acetate, and 2(3H)-furanone in all four media, with higher proportions of 5-hexenoic acid and CPL in Fe and Al than those in Cu and Zn media (Fig. 7). Being synthesized from CPL anionic ring-opening polymerization, PA depolymerization led to CPL as the major compound (Iwaya et al., 2006). Thus, the presence of CPL in aqueous phase was attributed to a series of depolymerization reactions in PA, including the cleavage of hydrogen bonds, hydrolysis, dehydration and cyclization reactions (Zhao et al., 2018). Additionally, 5-hexenoic acid can be derived from thermal degradation of CPL, so it serves as an instrumental indicator of PA degradation (Xu and Wang, 2022). In

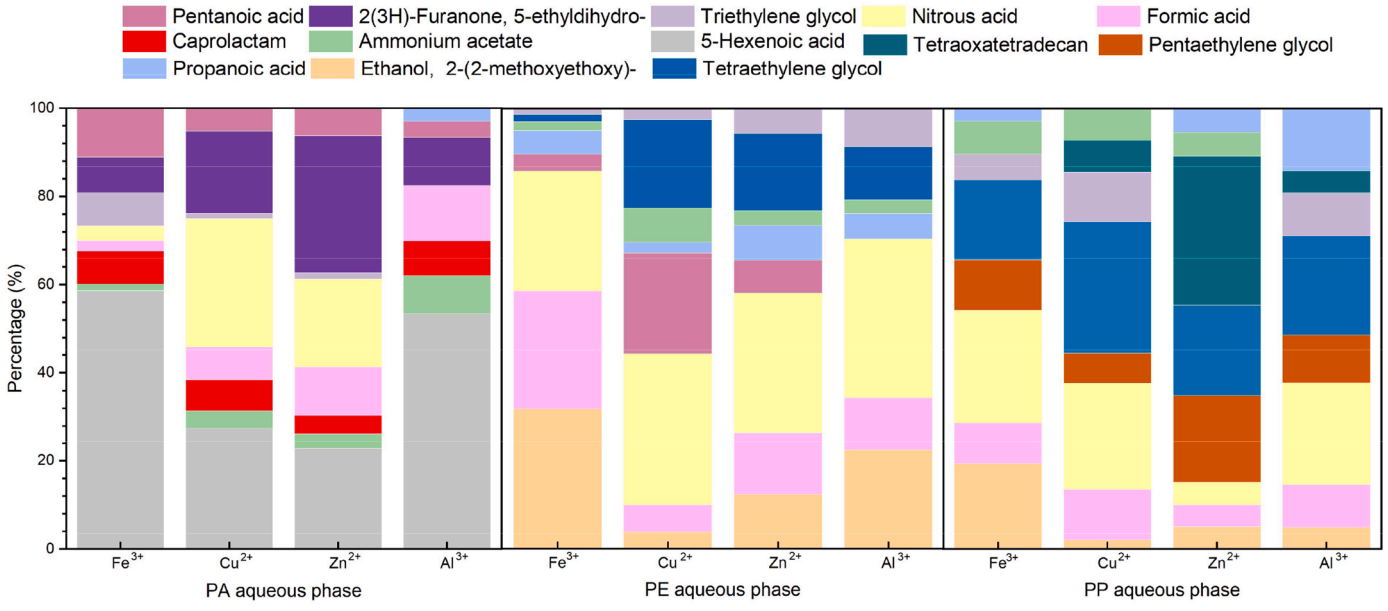

Fig. 7. GC–MS analysis for relative abundance of aqueous phase from HTP at 300 °C and 30 min.

contrast, due to the low degradation efficiency, the degradation products of PE and PP contained a low relative abundance of organic compounds (e.g. ethanol, tetraethylene glycol, and pentaethylene glycol) (Fig. 7) resulting from the cleavage of C—H bonds in the polymer chains and subsequent reactions with water under hydrothermal condition. It is evident that the relative abundance of degradation products plays a critical role in determining degradation efficiency, highlighting the necessity for a comprehensive understanding of the degradation mechanisms and product distribution of MPs.

Fig. 8 describes comparative percentages of products derived from Py GC–MS analyses of pristine MPs and solutes from HTP of MPs in different metallic media. The relative abundances of compounds from pyrolysis of pristine MPs (Table S2) and solutes (Table S3) were comprehensively compared to determine their relative percentages. Particularly, compounds detected in the solute from PA degradation displayed a high similarity with the pyrolytic products of pristine PA in all four media, especially the highest similarity up to 47% in Al media followed by Fe (26.7%), Cu (17.9%), and Zn (15.3%) media (Fig. 8a). Conversely, compounds in solutes from PE and PP degradation were only detected in Fe media, with the pyrolytic products similarity of 9.3% and 20.2% in PE and PP solute, respectively (Fig. 8b and c). These results were in good agreement with the degradation efficiency of MPs in the four media depicted in Fig. 5. Interestingly, this confirmed the presence of plastic materials in the solute with a size smaller than 26 μm, even nanoplastics (NPs) (dimensions ranging from 1 nm to 1 μm), which could be passed through the filter. Hence, HTP could depolymerize MPs into monomers and disintegrate them into smaller MPs and NPs.

This study indicates that GC–MS is reliable for analyzing volatile organic compounds from HTP of MPs in aqueous phase. However, smaller MPs and NPs are not fully analyzed. Py GC–MS could complement this by decomposing the remaining MPs and NPs into analyzable molecules, revealing the conversion of MPs to smaller forms. Nevertheless, these residues still pose persistence threats to the environment and human health, which is worthy of further investigation.

3.3. Degradation mechanisms for HTP of MPs in Fe^{3+}/Al^{3+}

Based on aforementioned data and discussion, potential degradation mechanisms for HTP of MPs in the most favorable Fe^{3+}/Al^{3+} media are proposed in Fig. 9. HTP at higher temperature generally reinforced the hydrolysis reaction to break down MPs substantially. Free radicals were concomitantly formed to further depolymerize and crack MPs to form intermediates throughout HTP (Jiang et al., 2022). Overall, MP degradation in HTP is mainly attributed to thermal hydrolysis reaction leading to chain scission of polymers, whereas Fe^{3+}/Al^{3+} ions are assumed to enhance free radical reaction rather than catalyzing the hydrolysis. Herein, the mechanism will mainly encompass the effect of Fe^{3+}/Al^{3+} ions on MPs degradation.

As depicted in Fig. 9a, the degradation of PA mainly involves free radical dissociation and nucleophilic substitution. Initially, hot-compressed subcritical water could induce unstable bonds in PA and generate free radicals to attack inter- and intra-molecular hydrogen bonds therein, resulting in cleavage of cross-linked structure and formation of linear polymers through free radical dissociation (Wang et al., 2017). Fe^{3+} and Al^{3+} could facilitate hydroxyl radical production to promote this reaction step (Salamone et al., 2013). Subsequently, the linear polymers were hydrolyzed to form aminocaproic acid with subcritical water assisted nucleophilic substitution. Ultimately, CPL, a primary ingredient in oils, was formed due to consecutive dehydration and cyclization of aminocaproic acid (Zhao et al., 2018). At the same time, continuous cracking and re-cracking of intermediates generated more free radical fragments to generate many secondary products via possible elimination and cyclization reactions (Zhao et al., 2018).

Similarly, Fe^{3+} ion has significantly catalyzed the degradation of PE and PP by promoting free radical dissociation to accelerate depolymerization. As shown in Fig. 9b and c, hydrothermal degradation mechanisms for PE and PP were briefly sketched according to one compratative study (Čolnik et al., 2021). PE depolymerization initially occurred to form long-chain hydrocarbon through free radical dissociation. Then, β–scission and hydrogen abstraction reaction occurred simultaneously to produce olefins and shorter-chain paraffins. Olefins could be converted to cycloparaffins, aromatics and alcohol via cyclization, aromatization and hydration reactions, respectively (Čolnik et al., 2021). Unlike PE, PP contains two types of C–C bonds, including the C—CH_3 bond (335 kJ/mol) and the –CH_2–CH_2– bond (348 kJ/mol), so its depolymerization sequence could be different. The C—CH_3, with a lower bond energy, is firstly scissored to form olefins by β-scission, followed by the cleavage of –CH_2–CH_2– bonds into paraffins and olefins through hydrogen abstraction and β-scission, respectively (Jin et al., 2020). Then, the follow-up degradation routes could be similar to that for PE.

4. Conclusions

This study has investigated HTP of MPs in subcritical water to elucidate the critical role of ubiquitous metal ions, especially Fe^{3+} and Al^{3+} ions, in facilitating hydrothermal degradation of MPs. Thermal hydrolysis reaction led to chain scission of polymers, so higher temperature favored the degradation of MPs. Decarboxylation and dehydration dominated the HTP of PA, whereas dehydration was more favorable for PE and PP. Limited weight loss was observed in HTP below 240 °C for all MPs. At 300 °C, weight loss for all MPs was increased by nearly four-fold. Nevertheless, the highest weight loss for PE and PP in water media was only 6.9% and 4.6%, respectively. Metal ions demonstrated a noticeable catalytic effect on hydrothermal degradation of MPs. In particular, Fe^{3+} was the most advantageous in degradation of

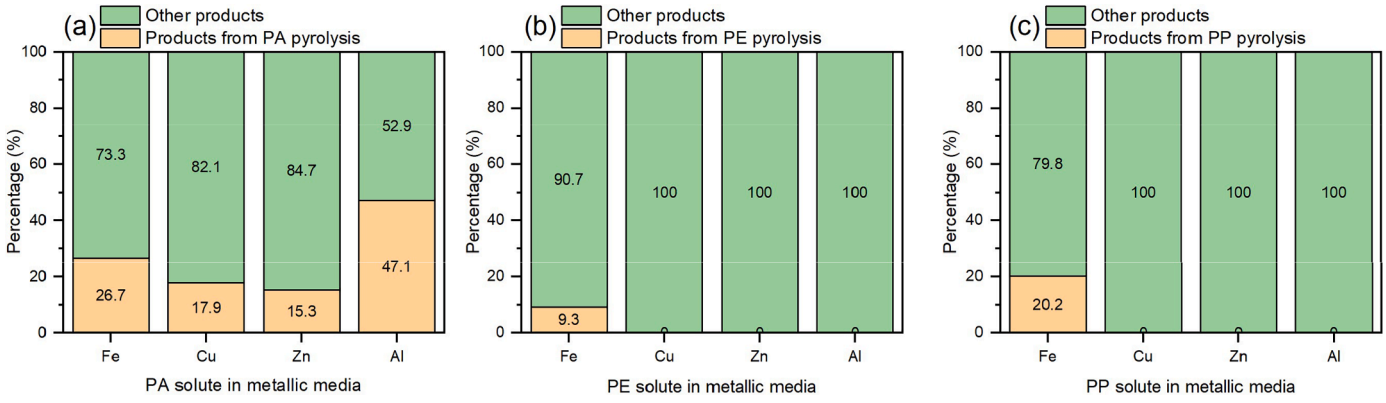

Fig. 8. Comparative percentages of products derived from Py GC–MS analysis of pristine MPs and solutes from HTP of (a) PA, (b) PE and (c) PP in different metallic media.

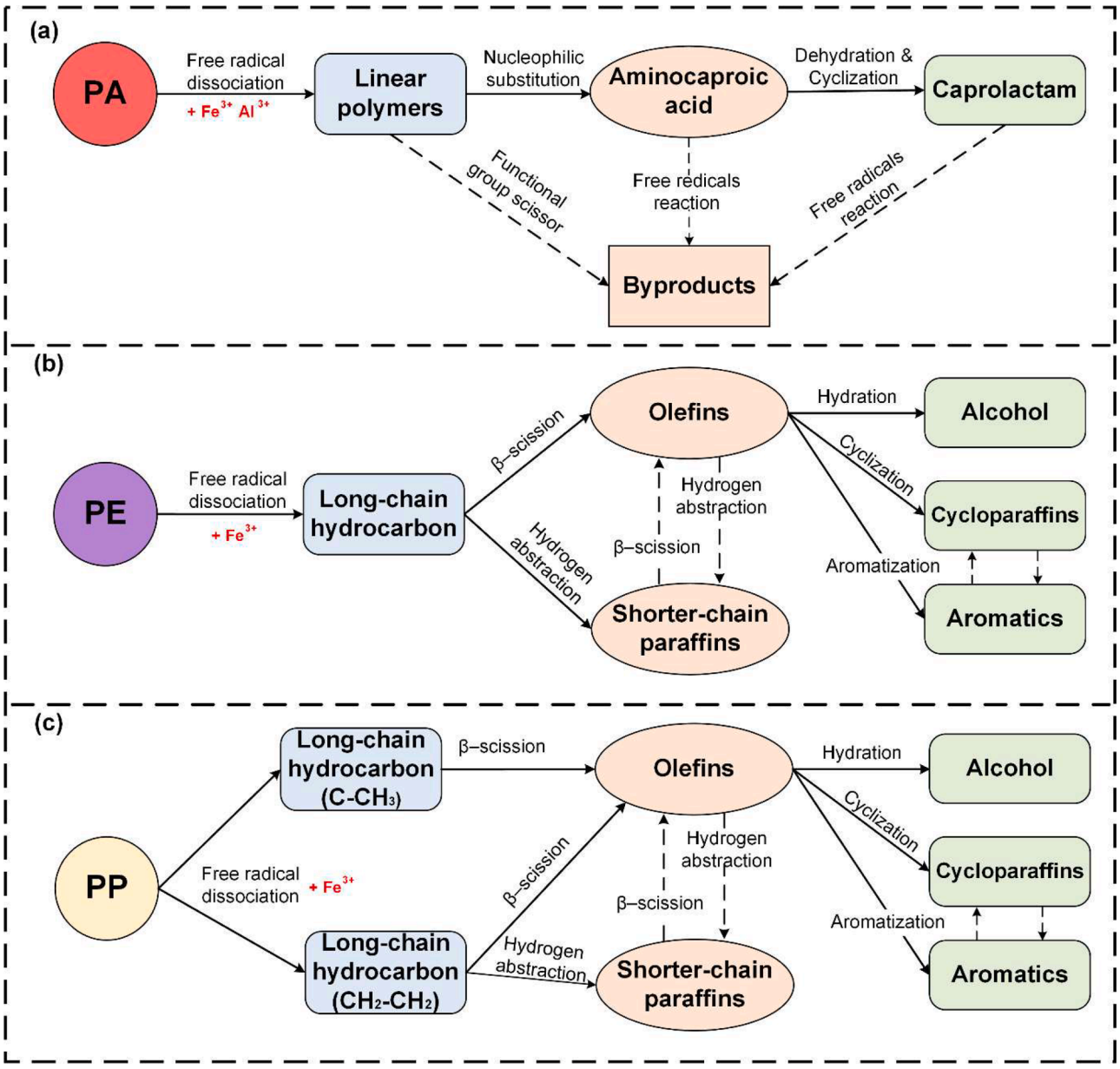

Fig. 9. Proposed degradation mechanisms for HTP of MPs in Fe^{3+}/Al^{3+} media.

all three MPs over Cu^{2+}, Zn^{2+} and Al^{3+}. Moreover, Fe^{3+} and Al^{3+} were supposed to enhance free radical reaction rather than catalyzing the hydrolysis. Thus, more hydroxyl radicals substantially facilitated PA degradation with a weight loss higher than 95% and 92% in Fe^{3+} and Al^{3+}, respectively. Likewise, Fe^{3+} distinctly catalyzed the depolymerization of PE and PP via enhanced free radical dissociation. More importantly, combined GC–MS and Py GC–MS analyses confirmed the conversion of MPs to smaller MPs and NPs via HTP, highlighting the great potential to recover value-added chemicals or monomers from plastics using HTP.

Declaration of Competing Interest

The authors declare the following financial interests/personal relationships which may be considered as potential competing interests:

Chao He reports financial support was provided by Research Council of Finland.

Data availability

Data will be made available on request.

Acknowledgments

We acknowledge the financial support from Tampere University, the Academy Research Fellowship and its related research project funded by Research Council of Finland (decision numbers: 341052, 346578).

Supplementary materials

Supplementary material associated with this article can be found, in the online version, at doi:10.1016/j.watres.2023.120672.

References

Alengebawy, A., Abdelkhalek, S.T., Qureshi, S.R., Wang, M.-Q., 2021. Heavy metals and pesticides toxicity in agricultural soil and plants: ecological risks and human health implications. Toxics 9, 42.

Apha, A., 2007. WEF (2005) Standard methods for the examination of water and wastewater.

Brennecke, D., Duarte, B., Paiva, F., Caçador, I., Canning-Clode, J., 2016. Microplastics as vector for heavy metal contamination from the marine environment. Estuar. Coast. Shelf Sci. 178, 189–195.

Cerruti, P., Carfagna, C., 2010. Thermal-oxidative degradation of polyamide 6, 6 containing metal salts. Polym. Degrad. Stab. 95, 2405–2412.

Chanaka Udayanga, W.D., Veksha, A., Giannis, A., Lisak, G., Chang, V.W.-C., Lim, T.-T., 2018. Fate and distribution of heavy metals during thermal processing of sewage sludge. Fuel 226, 721–744. https://doi.org/10.1016/j.fuel.2018.04.045.

Collivignarelli, M.C., Carnevale Miino, M., Caccamo, F.M., Milanese, C., 2021. Microplastics in sewage sludge: a known but underrated pathway in wastewater treatment plants. Sustain. 13, 12591 https://doi.org/10.3390/SU132212591.

Čolnik, M., Kotnik, P., Knez, Ž., Škerget, M., 2021. Hydrothermal decomposition of polyethylene waste to hydrocarbons rich oil. J. Supercrit. Fluids 169, 105136.

De-la-Torre, G.E., Dioses-Salinas, D.C., Castro, J.M., Antay, R., Fernández, N.Y., Espinoza-Morriberón, D., Saldaña-Serrano, M., 2020. Abundance and distribution of microplastics on sandy beaches of Lima, Peru. Mar. Pollut. Bull. 151, 110877 https://doi.org/10.1016/J.MARPOLBUL.2019.110877.

Dioses-Salinas, D.C., Pizarro-Ortega, C.I., De-la-Torre, G.E., 2020. A methodological approach of the current literature on microplastic contamination in terrestrial environments: current knowledge and baseline considerations. Sci. Total Environ. 730, 139164 https://doi.org/10.1016/J.SCITOTENV.2020.139164.

Dümichen, E., Eisentraut, P., Bannick, C.G., Barthel, A.-K., Senz, R., Braun, U., 2017. Fast identification of microplastics in complex environmental samples by a thermal degradation method. Chemosphere 174, 572–584.

Ellis, L.D., Rorrer, N.A., Sullivan, K.P., Otto, M., McGeehan, J.E., Román-Leshkov, Y., Wierckx, N., Beckham, G.T., 2021. Chemical and biological catalysis for plastics recycling and upcycling. Nat. Catal. 4, 539–556.

Gao, F., Li, J., Sun, C., Zhang, L., Jiang, F., Cao, W., Zheng, L., 2019. Study on the capability and characteristics of heavy metals enriched on microplastics in marine environment. Mar. Pollut. Bull. 144, 61–67. https://doi.org/10.1016/j.marpolbul.2019.04.039.

Geng, H., Xu, Y., Zheng, L., Gong, H., Dai, L., Dai, X., 2020. An overview of removing heavy metals from sewage sludge: achievements and perspectives. Environ. Pollut. 266, 115375.

Han, L., Zhang, B., Li, D., Chen, L., Feng, Y., Xue, L., He, J., Feng, Y., 2022. Co-occurrence of microplastics and hydrochar stimulated the methane emission but suppressed nitrous oxide emission from a rice paddy soil. J. Clean. Prod. 337, 130504 https://doi.org/10.1016/J.JCLEPRO.2022.130504.

Hu, K., Zhou, P., Yang, Y., Hall, T., Nie, G., Yao, Y., Duan, X., Wang, S., 2021. Degradation of Microplastics by a Thermal Fenton Reaction. ACS ES&T Engineering.

Iñiguez, M.E., Conesa, J.A., Fullana, A., 2019. Hydrothermal carbonization (HTC) of marine plastic debris. Fuel 257, 116033. https://doi.org/10.1016/j.fuel.2019.116033.

Iwaya, T., Sasaki, M., Goto, M., 2006. Kinetic analysis for hydrothermal depolymerization of nylon 6. Polym. Degrad. Stab. 91, 1989–1995. https://doi.org/10.1016/j.polymdegradstab.2006.02.009.

Jiang, C., Chen, Z., Lu, B., Li, Z., Zhang, S., Liu, Y., Luo, G., 2022. Hydrothermal pretreatment reduced microplastics in sewage sludge as revealed by the combined micro-Fourier transform infrared (FTIR) and Raman imaging analysis. Chem. Eng. J. 450, 138163.

Jin, K., Vozka, P., Gentilcore, C., Kilaz, G., Wang, N.-H.L., 2021. Low-pressure hydrothermal processing of mixed polyolefin wastes into clean fuels. Fuel 294, 120505. https://doi.org/10.1016/j.fuel.2021.120505.

Jin, K., Vozka, P., Kilaz, G., Chen, W.-T., Wang, N.-H.L., 2020. Conversion of polyethylene waste into clean fuels and waxes via hydrothermal processing (HTP). Fuel 273, 117726.

Li, W., Meng, J., Zhang, Y., Haider, G., Ge, T., Zhang, H., Li, Z., Yu, Y., Shan, S., 2022a. Co-pyrolysis of sewage sludge and metal-free/metal-loaded polyvinyl chloride (PVC) microplastics improved biochar properties and reduced environmental risk of heavy metals. Environ. Pollut. 302, 119092.

Li, X., Chen, L., Mei, Q., Dong, B., Dai, X., Ding, G., Zeng, E.Y., 2018. Microplastics in sewage sludge from the wastewater treatment plants in China. Water Res. 142, 75–85. https://doi.org/10.1016/J.WATRES.2018.05.034.

Li, X., Wang, X., Chen, L., Huang, X., Pan, F., Liu, L., Dong, B., Liu, H., Li, H., Dai, X., 2022b. Changes in physicochemical and leachate characteristics of microplastics during hydrothermal treatment of sewage sludge. Water Res. 222, 118876.

Luo, H., Zhao, Y., Li, Y., Xiang, Y., He, D., Pan, X., 2020. Aging of microplastics affects their surface properties, thermal decomposition, additives leaching and interactions in simulated fluids. Sci. Total Environ. 714, 136862 https://doi.org/10.1016/j.scitotenv.2020.136862.

Lusher, A.L., Burke, A., O'Connor, I., Officer, R., 2014. Microplastic pollution in the Northeast Atlantic Ocean: validated and opportunistic sampling. Mar. Pollut. Bull. 88, 325–333. https://doi.org/10.1016/J.MARPOLBUL.2014.08.023.

Ma, D., Liang, L., Hu, E., Chen, H., Wang, D., He, C., Feng, Q., 2021. Dechlorination of polyvinyl chloride by hydrothermal treatment with cupric ion. Process Saf. Environ. Prot. 146, 108–117.

Mahon, A.M., O'Connell, B., Healy, M.G., O'Connor, I., Officer, R., Nash, R., Morrison, L., 2017. Microplastics in sewage sludge: effects of treatment. Environ. Sci. Technol. 51, 810–818.

Mao, R., Hu, Y., Zhang, S., Wu, R., Guo, X., 2020. Microplastics in the surface water of Wuliangsuhai Lake, northern China. Sci. Total Environ. 723, 137820 https://doi.org/10.1016/J.SCITOTENV.2020.137820.

Ni, B.-J., Zhu, Z.-R., Li, W.-H., Yan, X., Wei, W., Xu, Q., Xia, Z., Dai, X., Sun, J., 2020. Microplastics mitigation in sewage sludge through pyrolysis: the role of pyrolysis temperature. Environ. Sci. Technol. Lett. 7, 961–967.

Pannase, A.M., Singh, R.K., Ruj, B., Gupta, P., 2020. Decomposition of polyamide via slow pyrolysis: effect of heating rate and operating temperature on product yield and composition. J. Anal. Appl. Pyrolysis 151, 104886. https://doi.org/10.1016/j.jaap.2020.104886.

Pöykiö, R., Watkins, G., Dahl, O., 2019. Characterisation of municipal sewage sludge as a soil improver and a fertilizer product. Ecol. Chem. Eng. 26, 547–557.

Raju, S., Carbery, M., Kuttykattil, A., Senthirajah, K., Lundmark, A., Rogers, Z., Suresh, S., Evans, G., Palanisami, T., 2020. Improved methodology to determine the fate and transport of microplastics in a secondary wastewater treatment plant. Water Res. 173, 115549.

Ro, K.S., Libra, J.A., Alvarez-Murillo, A., 2020. Comparative studies on water-and vapor-based hydrothermal carbonization: process analysis. Energies 13, 5733.

Salamone, M., Mangiacapra, L., DiLabio, G.A., Bietti, M., 2013. Effect of metal ions on the reactions of the cumyloxyl radical with hydrogen atom donors. Fine control on hydrogen abstraction reactivity determined by Lewis acid–base interactions. J. Am. Chem. Soc. 135, 415–423. https://doi.org/10.1021/ja309579t.

Torres, F.G., Dioses-Salinas, D.C., Pizarro-Ortega, C.I., De-la-Torre, G.E., 2021. Sorption of chemical contaminants on degradable and non-degradable microplastics: recent progress and research trends. Sci. Total Environ. 757, 143875.

Wang, H.-F., Qi, H.-Y., Du, K., Ran, D.-D., Liu, W.-H., Shen, X.-F., Zeng, R.J., 2022b. Reinterpretation of the mechanism of coagulation and its effects in waste activated sludge treatment. Sep. Purif. Technol. 291, 120958 https://doi.org/10.1016/j.seppur.2022.120958.

Wang, W., Meng, L., Yu, J., Xie, F., Huang, Y., 2017. Enhanced hydrothermal conversion of caprolactam from waste monomer casting polyamide over H-Beta zeolite and its mechanism. J. Anal. Appl. Pyrolysis 125, 218–226.

Wang, X., Zhang, R., Li, Z., Yan, B., 2022a. Adsorption properties and influencing factors of Cu(II) on polystyrene and polyethylene terephthalate microplastics in seawater. Sci. Total Environ. 812, 152573 https://doi.org/10.1016/J.SCITOTENV.2021.152573.

Wang, X., Zhou, W., Liang, G., Song, D., Zhang, X., 2015. Characteristics of maize biochar with different pyrolysis temperatures and its effects on organic carbon, nitrogen and enzymatic activities after addition to fluvo-aquic soil. Sci. Total Environ. 538, 137–144.

Xu, G., Wang, Q., 2022. Chemically recyclable polymer materials: polymerization and depolymerization cycles. Green Chem. 24, 2321–2346.

Xu, Z., Bai, X., 2022. Microplastic degradation in sewage sludge by hydrothermal carbonization: efficiency and mechanisms. Chemosphere 297, 134203.

Xue, Y., Johnston, P., Bai, X., 2017. Effect of catalyst contact mode and gas atmosphere during catalytic pyrolysis of waste plastics. Energy Convers. Manag. 142, 441–451. https://doi.org/10.1016/j.enconman.2017.03.071.

Yin, J., Li, G., He, W., Huang, J., Xu, M., 2011. Hydrothermal decomposition of brominated epoxy resin in waste printed circuit boards. J. Anal. Appl. Pyrolysis 92, 131–136.

Zhao, X., Xia, Y., Zhan, L., Xie, B., Gao, B., Wang, J., 2018. Hydrothermal treatment of e-waste plastics for tertiary recycling: product slate and decomposition mechanisms. ACS Sustain. Chem. Eng. 7, 1464–1473.